Mineralogical Magazine, February 1999, Vol. 63(1), pp. 1–12

Rapid exsolution behaviour in the bornite–digenite series, and implications for natural ore assemblages

B. A. GRGURIC*

Department of Earth Sciences, University of Cambridge, Downing Street, Cambridge CB2 3EQ, UK

AND

A. PUTNIS

Institut für Mineralogie, Universität Münster, Corrensstrasse 24, D-48149 Münster, Germany

ABSTRACT

Intermediate compositions along the bornite–digenite join exsolve during quenching from above-solvus temperatures. This involves vacancy clustering and cation ordering processes, and is facilitated by fast cation diffusion rates in the presence of a large (10–25%) metal vacancy population. Samples of six different compositions across the bornite–Cu_9S_5 join, synthesised from component elements in sealed quartz capsules, were water-quenched from 600°C and analysed using high-resolution neutron powder diffraction (HRPD). Time-of-flight spectra measured at room temperature showed all intermediate compositions had exsolved into mixtures of bornite and low digenite with a $5.0a$ superstructure. No evidence for the presence of any other phase was found. Variations in the lattice parameters of the exsolved bornite phase were observed for different bulk compositions across the join, and ascribed to variations in the degree of order. Bornite exsolved from digenite-rich compositions may not be fully ordered due to the much lower solvus temperatures at the Cu-rich end of the solid solution. As only slight differences were observed between the diffraction patterns of a visibly exsolved and a rapidly quenched sample of the same bulk composition, the formation of optically-visible exsolution lamellae on {100} is ascribed to a process of coalescence of sub-microscopic domains initially formed during the quenching process. The rapid kinetics of exsolution at geologically low temperatures, explains the lack of authenticated natural occurrences of intermediate compositions in the solid solution in nature, and the limited degree of stoichiometric variation observed in end-members.

KEYWORDS: bornite, digenite, exsolution, cation ordering.

Introduction

EXSOLUTION in sulphide minerals is a geologically important process, instrumental in the formation of many distinctive ore textures (Ramdohr, 1969). The characterisation of exsolution behaviour in ore minerals can have applications to understanding ore depositional processes, and in particular the thermal history of mineral assemblages following deposition. Unlike many silicate minerals however, most common ore mineral assemblages are not suitable for the characterisation of P, T, X_{fluid} conditions at the time of deposition owing to their rapid transformation kinetics. This allows the assemblage to re-equilibrate texturally and mineralogically in pace with typical geological cooling rates, or under mild metamorphism (Barton, 1970). The sulphides in the Cu-Fe-S system are particularly susceptible to these types of modifications at low temperatures, with several high-temperature phases not capable of being quenched in laboratory experiments (Morimoto and Kullerud, 1961; Barton and Skinner, 1979). We report on an extreme case of rapid exsolution behaviour exhibited by intermediate compositions of the extensive bornite (Cu_5FeS_4)–digenite

---

* Present address: WMC Mount Keith Operations, P.O. Box 238, Welshpool Delivery centre, W.A. 6986, Australia

($Cu_{8.63}Fe_{0.13}S_5$) solid solution series. The interactions between cation/vacancy ordering, associated structural transitions, superstructuring, and exsolution in this series have proved a fruitful source of investigation for several decades (Kullerud, 1960; Morimoto and Kullerud, 1966; Pierce and Buseck, 1978; Grguric *et al.*, 1998). With some exceptions most of the numerous studies have been focused on the end-members, with the result that the structural systematics of the intermediate part of the solid solution are still incomplete. A detailed examination of these compositions is now timely.

The aim of this work is to present high-resolution neutron powder diffraction data on a series of synthetic samples across the bornite–digenite solid solution, demonstrating the unexpectedly rapid kinetics of exsolution in this system.

The bornite–digenite series

Bornite and digenite exhibit a complete solid solution above approximately 330°C, according to the phase diagram of Kullerud (1960). Both these end-members of the solid solution are economically important ores of copper, and are commonly observed in close association in deposits formed in a wide spectrum of geological conditions. These range from high-temperature magmatic ores, where sulphides segregate as an immiscible liquid phase, to supergene enrichment zones formed via precipitation from meteoric waters at near ambient conditions. Most economically important deposits containing these minerals are formed by hydrothermal processes at temperatures between 150 and 300°C however, allowing the possibility of the deposition of solid solutions of the end-members.

The structure of the solid solution at above-solvus temperatures is cubic (*Fm*3*m*), the unit cell ($a \approx 5.5-5.6$ Å) consisting of a cubic close-packed framework of sulphur atoms (Kanazawa *et al.*, 1978). The 8 tetrahedral interstices of this sulphur framework contain a random distribution of Cu and Fe atoms and vacancies, with a metal vacancy population varying from 10% in digenite to 25% in bornite, while corresponding Cu:Fe ratios vary from 5:1 to 89:1.

At 270°C the bornite end-member undergoes a tricritical phase transition on cooling to an intermediate form involving a combination of vacancy clustering and cation ordering (Grguric *et al.*, 1998). This results in an 3 dimensional alternation of anti-fluorite and zinc-blende structured *a* subcells, giving a 2*a* supercell (Kanazawa *et al.*, 1978). This is followed by a strongly first-order transition, associated with doubling of the cell in the *b*-direction, which begins between 200 and 150°C depending on the degree of order attained during cooling in the intermediate phase (Grguric *et al.*, 1998). The resultant low bornite structure has an orthorhombic (*Pbca*; pseudo-tetragonal) 2*a*4*a*2*a* supercell (Koto and Morimoto, 1975), and the transition to this form is believed to result from short-range vacancy ordering in the anti-fluorite-structured subcells (Koto and Morimoto, 1975; Pierce and Buseck, 1978). Low bornite is the only polymorph known to occur in nature.

The phase relations near the Cu_9S_5-end of the join are considerably more complex and the characterisation of assemblages is often complicated by the presence of metastable phases (Roseboom, 1966; Morimoto and Koto, 1970; Pósfai and Buseck, 1994). Low digenite *sensu strictu* has been defined by Morimoto and Gyobu (1971) as a cubic (*Fm*3*m*) phase possessing an integer 5*a* superstructure, as observed in natural samples. In defining the single-phase compositional field of low digenite in Cu-Fe-S space, these workers found that substitution of 0.4–1.6 atom % Fe for Cu (as measured in natural digenites) was required to stabilise the 5*a* superstructure. They referred to this compositional field, which includes a small range of compositions along the bornite–Cu_9S_5 join centred near 12 mol.% bornite (Fig. 1), as the

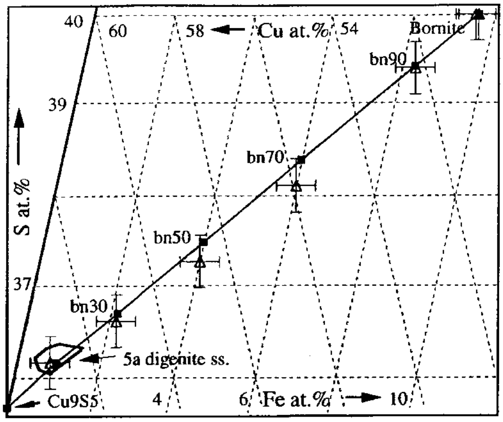

FIG. 1. Ideal (filled squares) and measured (triangles) bulk compositions of samples along the bornite-Cu_9S_5 join used in this study plotted in Cu-Fe-S space. Limits of the 5*a*-digenite solid solution as determined by Morimoto and Gyobu (1971) are indicated.

'digenite-solid solution'. Morimoto and Gyobu (1971) denoted the remainder of the join between the digenite solid solution and Cu_9S_5, the 'digenite-type' solid solution. This was found to consist of digenite-type phases with apparent non-integer supercells (between 5.1 and 6.0*a*), which were metastable relative to mixtures of 5*a*-digenite, djurleite and anilite. Both the transition behaviour and the detailed structure of the low digenite polymorph are poorly characterised, however the transition from the high phase, which occurs at 78–82°C, resembles the high-intermediate transition in bornite, especially with regards to the structural modification involved (1*a*-type $Fm3m \rightarrow$ 5a-type $Fm3m$; Morimoto and Gyobu, 1971), and the lack of thermal hysteresis (Grguric *et al.*, 1998).

Intermediate compositions along the bornite–Cu_9S_5 join have been examined by Brett (1964), and Morimoto and Kullerud (1966). Brett annealed 12 intermediate compositions at 350°C for several weeks, then examined these samples optically after cooling to 50°C over timescales varying from 6.5 minutes to 130 days. In many cases exsolution textures of various types were observed, mainly in bulk compositions towards the bornite end-member. No attempt at a characterisation of the exsolved phases was made however. Morimoto and Kullerud (1966) used single-crystal X-ray techniques to examine compositions spanning the entire solid solution. They noted the presence of various metastable superstructures of the high form in crystals freshly quenched from above-solvus temperatures. Their fine-scale twinning hypothesis for the formation of these superstructures has been shown to be untenable for both end-members on the basis of TEM evidence (Putnis and Grace, 1976; Pierce and Buseck, 1978; van Dyck *et al.*, 1980) and may therefore be inapplicable to the remainder of the solid solution. In bulk compositions between bornite and the digenite solid solution Morimoto and Kullerud observed that the metastable superstructures decomposed to mixtures of low bornite and digenite, but this process was not elaborated on.

Experimental

Sample preparation

Six compositions along the Cu_5FeS_4–Cu_9S_5 join were used in this study: bn_{100}, bn_{90}, bn_{70}, bn_{50}, bn_{30} and dg_{100}. The dg_{100} sample had some Fe substituted for Cu to place the sample in the stable digenite field (Fig. 1). With the exception of one bn_{100} sample which was natural, each bulk composition was synthesised in a single 6 gram batch. Synthesis involved heating carefully weighed quantities of high purity (Aldrich 99.999%) elemental Cu, Fe and S in vacuum-sealed silica-glass capsules. A length of silica-glass rod and silica wool was also included in each capsule to minimise the amount of vacuum space and insulate the charge during sealing. After initial reaction at 400°C for 24 hours followed by heating at 950°C for 5 days, the capsules were slowly cooled over 24 hours, broken open, and the charges ground, with the entire grinding process being carried out under acetone to inhibit oxidation. These charges were then resealed in silica-glass capsules and heated at 900°C for a further 14 days to homogenise the sulphide. The capsules were then slowly cooled to 600°C, and then quenched in cold water. Cooling to 600°C is necessary to prevent excessive condensation of elemental sulphur on the walls of the capsule on quenching, which can result in a serious modification of the bulk composition of the charge. The synthetic products, as verified by reflected light microscopy, were homogeneous semi-cylindrical masses of coarsely polycrystalline sulphide. The tendency of Cu-rich sulphide charges to 'wet' the walls of the silica capsules at high temperatures meant that heat transfer during quenching was greatly enhanced. Grain-sizes of individual crystals were 1 to 5 mm. Despite the large charge size, the samples were shown to be homogeneous and of approximately correct bulk composition by electron microprobe operating in WDS mode (Table 1). Although a comparison with ideal compositions along the bornite–Cu_9S_5 join (Fig. 1) show the mean data to have a slight sulphur deficiency, all the data points lie on the ideal line within the error of the analysis. No evidence of exsolution could be found during either optical or scanning electron microscopic examination.

The sample of bn_{90} composition was annealed under vacuum in a sealed Pyrex capsule for 11 weeks at 180°C and then water-quenched. Examination of polished sections of this sample in reflected light, showed it to be visibly exsolved, exhibiting the characteristic 'basket-weave' microstructure due to the formation of bornite lamellae on {100} planes of the matrix (Fig. 2). This sample was then ground and sealed under vacuum as described below.

TABLE 1. Compositions of samples used in this study, measured by WDS microprobe (averages of 10 analyses). All formulae are presented normalised to 5 sulphurs. Mineralogy of these samples was obtained from neutron diffraction data in Fig. 3

Sample	Origin	Cu (wt.%)*	Fe (wt.%)	S (wt.%)	Formula	Phases present @ room *T*
bn_{100}	Magma Mine, Arizona	63.38	10.96	25.55	$Cu_{6.26}Fe_{1.24}S_{5.00}$	2*a*4*a*2*a*-bn + trace dg
bn_{100}	synthetic	63.31	11.13	25.56	$Cu_{6.25}Fe_{1.25}S_{5.00}$	2*a*4*a*2*a*-bn
bn_{90}	synthetic	65.38	9.58	25.05	$Cu_{6.59}Fe_{1.10}S_{5.00}$	2*a*4*a*2*a*-bn + 5.0*a*-dg
bn_{70}	synthetic	68.86	6.80	23.81	$Cu_{7.30}Fe_{0.82}S_{5.00}$	2*a*4*a*2*a*-bn + 5.0*a*-dg
bn_{50}	synthetic	71.08	4.46	22.84	$Cu_{7.85}Fe_{0.56}S_{5.00}$	2*a*4*a*2*a*-bn + 5.0*a*-dg
bn_{30}	synthetic	74.37	2.48	22.54	$Cu_{8.33}Fe_{0.32}S_{5.00}$	2*a*4*a*2*a*-bn + 5.0*a*-dg
dg_{100}	synthetic	76.76	0.94	22.25	$Cu_{8.70}Fe_{0.12}S_{5.00}$[†]	5.0*a*-dg

* Chalcocite (Cu_2S) standard used for Cu; pyrite (FeS_2) for Fe and S.

[†] This composition chosen as it gives a stable 5*a* superlattice in the low phase (Morimoto and Gyobu, 1971).

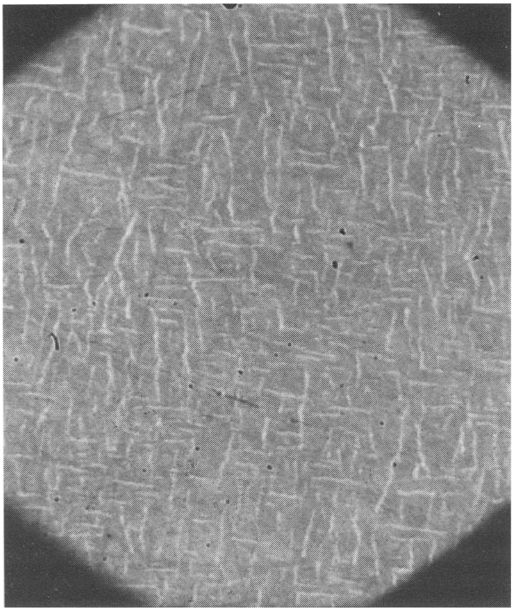

FIG. 2. Photomicrograph of the annealed sample of composition bn_{90} taken in reflected light, showing the characteristic 'basket-weave' microstructure defined by digenite lamellae. Observed proportions of bornite and digenite mirror the bulk composition. Field of view is 75 μm.

Neutron diffraction

Approximately 2 cm^3 of each sample composition was used for neutron diffraction analysis. After being ground under acetone in an agate mortar and pestle, the powder was sealed under vacuum together with a silica wool plug in high-purity Spectrosil® silica-glass capsules. Diffraction measurements were performed on the high-resolution neutron powder diffractometer (HRPD) at the ISIS spallation source, Oxfordshire (Johnson and David, 1985; Ibberson *et al.*, 1992). The sample capsules were inserted into 1 cm internal diameter Harwell-type cylindrical vanadium sample cans and fitted to the central stick of the diffractometer.

Room-temperature data collection was performed in runs of up to 1.7 h duration giving an integrated neutron flux of 100 mA. Diffraction data were collected in two neutron time-of-flight (TOF) windows spanning 35–120 ms and 85–165 ms, corresponding to *d*-spacing ranges of 0.72–2.49 Å and 1.76–3.42 Å respectively. Conversion from TOF in ms to *d*-space in Å is performed by multiplication by a factor of 2.07182×10^{-2}. All measurements were made with the diffractometer at the 1 metre position, resulting in an intrinsic resolution of $\Delta d/d = 8 \times 10^{-4}$ over the entire TOF range (Knight, 1996). The exceptionally high resolution of this instrument was the key factor in enabling diffraction peaks of coexisting bornite and digenite to be positively distinguished. The data were normalised to the incident neutron spectrum, and the background subtraction and detector efficiency corrections made using the program VA_COR (Ibberson *et al.*, 1992) which utilises a diffraction pattern of metallic vanadium. Peak positions and intensities were measured using the ISIS program PRGFIT, and cell parameters were obtained using the program UnitCell by Holland and Redfern (1997).

For all intermediate compositions, several days to weeks had elapsed between quenching and analysis on HRPD during which the samples were stored at 5°C. In order to compare the diffraction patterns of freshly quenched and visibly exsolved intermediate solid solution, room-temperature diffraction data were collected for the annealed and exsolved bn_{90} sample, after which the capsule was removed from the diffractometer and heated at 450°C for 4 hours. The capsule was then quenched and diffraction data collected again immediately. Our previous experiments have shown that above-solvus annealing for this length of time is sufficient to completely re-homogenise the visible microstructure in samples of this composition, and that the 1*a*-solid solution is the only phase present in *in-situ neutron* diffraction runs on bn_{90} above 232°C (Grguric, Harrison and Putnis, in prep.).

Results and discussion

Exsolution

Neutron powder diffraction patterns spanning the entire solid solution are shown in Fig. 3. These were collected at room-*T* and, with the exception of the bn_{90} sample and the natural bornite, all runs had been quenched from 600°C. The important feature of these patterns is that all quenched intermediate compositions can be seen to be exsolved into two-phase mixtures of bornite and digenite. This is most clearly seen in the region around 90 ms where the (10,10,0) digenite peak and the (084) bornite peak (both corresponding to the (220) peak of the 1*a*-solid solution) are well resolved. The positions of respective bornite and

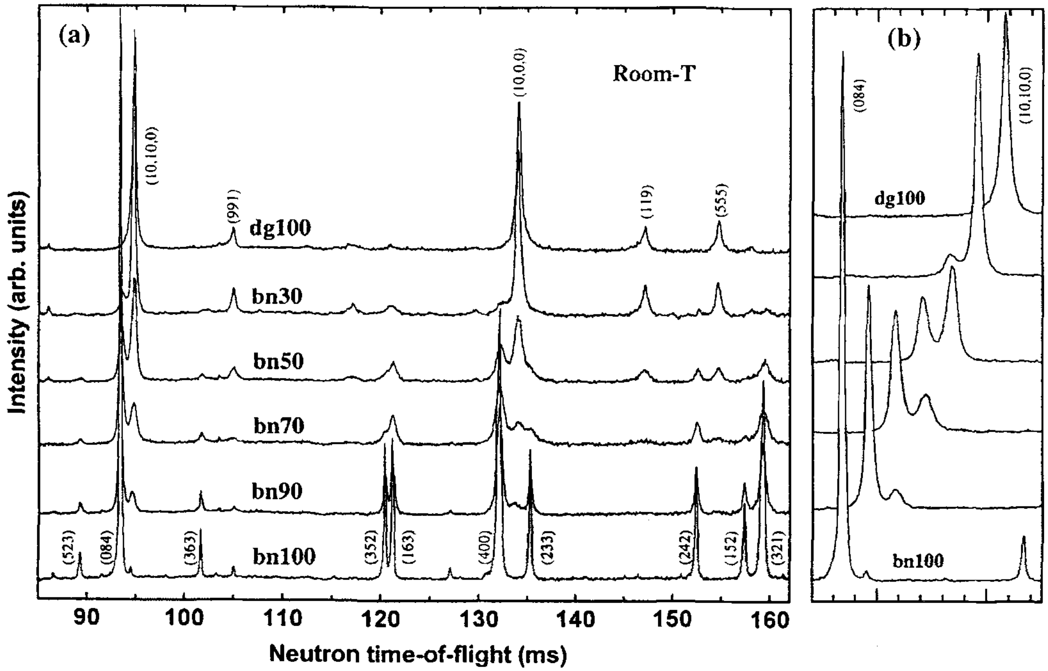

FIG. 3. (*a*) Neutron powder diffraction patterns (85–165 ms window) collected at room-*T* of samples with compositions spanning the bornite-digenite join. All samples with the exception of bn_{100} are synthetic and have been water-quenched from 600°C. Bn_{90} sample has been quenched from 450°C. (*b*) Expanded view of the 92–102 ms section of (a), displaced along a third composition axis, showing the intensity variation of digenite (10,10,0) and bornite (084) peaks. Note presence of trace digenite component in natural (Magma Mine) bornite sample.

digenite peaks occur at similar values of TOF across the compositional range (Fig. 5), and the peak intensity variation with composition mirrors the change in molar proportions of the end-members (Fig. 6), suggesting the exsolution process is essentially complete.

The dg_{100} sample and the exsolved digenite phase present in intermediate samples quenched from 600°C exhibit sub-cell lattice parameters which correspond to the compositional field of the stable 5*a*-superstructured form (Morimoto and Gyobu, 1971). All these samples showed the characteristic digenite (991) and (119) superlattice reflections. The positions of these peaks are not shifted (within error) from their calculated position for a 5.0*a*-superlattice based on the sublattice peak positions, implying the digenite phase present in all these samples is low digenite and thus is stable relative to other Cu-S phases (Morimoto and Gyobu, 1971).

Despite the aforementioned slight compositional deviations from the join of three of the intermediate samples (Fig. 1), no other phase could be detected in the diffraction patterns. Furthermore there is no evidence in the diffraction data of peaks corresponding to the various metastable non-end-member supercells described by Morimoto and Kullerud (1966). With increasing digenite content the quenched solid solution does show evidence of non-equilibrium behaviour however, which can be seen in the bornite lattice parameters of samples with bornite contents of 30 and 50 mole percent (Fig. 4), and in the major peak positions across the solid solution (Fig. 5). In these samples the bornite *a* cell-edge can be seen to rise progressively with increasing digenite content, and in bn_{30} *a* is greater than *c* (Table 2), in contrast to ordered end-member bornite. We attribute this to the sluggish ordering kinetics in the exsolved bornite phase which, despite the rapid exsolution kinetics, can retain quenched-in disorder in the intermediate structure (Kanazawa *et al.*, 1978; Grguric *et al.*, 1998). Owing to the consolute

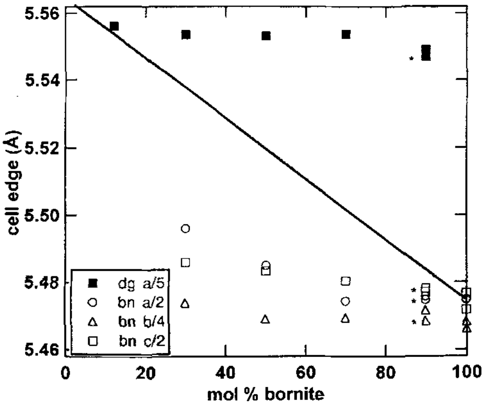

FIG. 4. Lattice parameters of coexisting bornite and digenite at room-*T*, plotted as a function of the bulk compositions of the starting material. Data have been scaled (see legend) for comparative purposes. Asterisks distinguish annealed bn_{90} sample measurements from quenched sample. Bold line refers to cell-edge of the fundamental subcell for homogeneous samples across the solid solution (data from Morimoto and Kullerud, 1966). Data at 12 mol.% bornite corresponds to digenite proper (see Fig. 1).

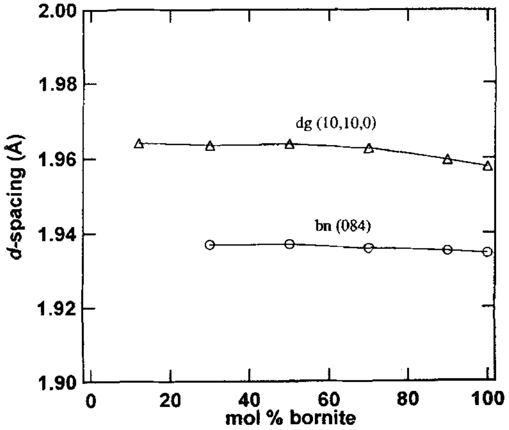

FIG. 5. Variation in *d*-spacing with bulk composition for coexisting bornite and digenite {220} peaks at room-*T*, indexed to the relevant low supercells. Digenite data at 100 mol.% bn refers to position of trace digenite peak seen in Magma Mine bornite sample in Fig. 3. Bn_{90} sample has been quenched from 450°C and all other samples were quenched from 600°C.

point of the solvus being offset towards the bornite end-member (Kullerud, 1960; Kullerud and Morimoto, 1966) digenite-rich bulk compositions have lower solvus temperatures relative to more bornite-rich bulk compositions. Our thermal and *in situ* neutron diffraction experiments (Grguric, Harrison and Putnis, in prep.) have shown, in contradiction to the original Kullerud phase diagram, that for bulk compositions of 30 and 50 mole percent bornite the solvus lies at 84° and 160°C respectively. Thus on quenching, bn_{30} remains in the single-phase 1*a*-solid solution field until the sample temperature falls to 84°C, while more bornite-rich compositions begin exsolution and ordering at higher temperatures (e.g. 232°C for bn_{90}), and experience greater undercooling below the solvus. Both these factors militate against an identical degree of order being attained in the bornite phase on rapid quenching solid solution compositions across the join. However the considerably lower cooling rates following deposition in ore-forming systems would probably allow the ordering process to attain equilibrium. The remarkable aspect of this solid solution, when the low solvus temperatures of intermediate digenite-rich compositions are taken into account, is the fact that exsolution into a two-phase mixture occurs during rapid quenching alone, as is clear from a comparison of our measured lattice parameter data with the sub-cell edge of single phase compositions across the join (Fig. 4). This implies the existence of a strong thermodynamic driving force for exsolution, and that the kinetics of nucleation of bornite and

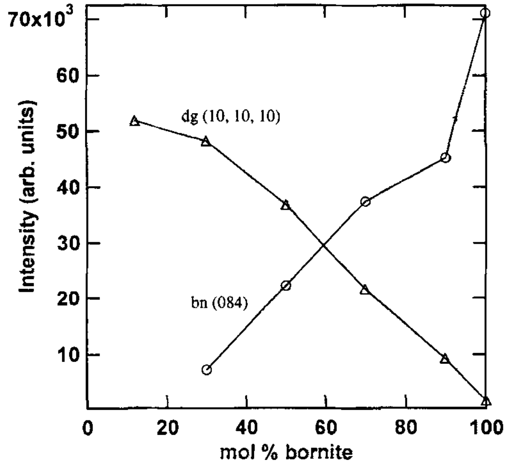

FIG. 6. Intensity variation of bornite and digenite Bragg peaks across the solid solution. Data collected from quenched samples at room-*T*.

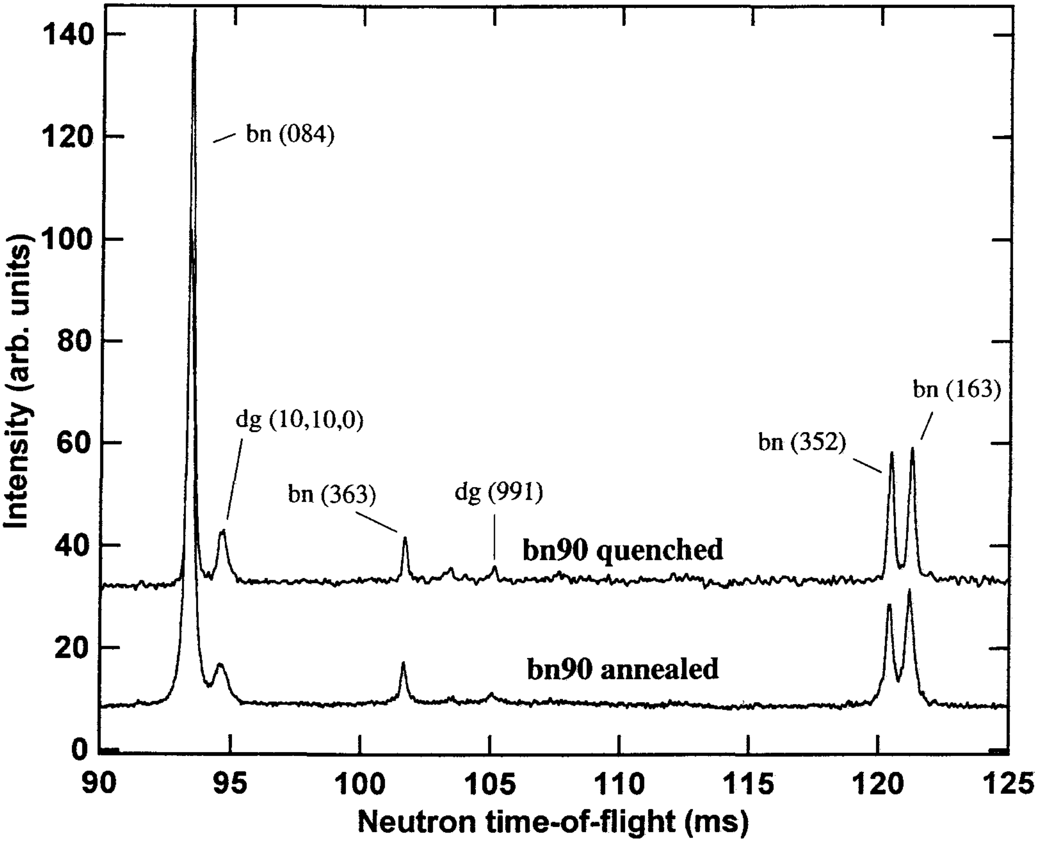

FIG. 7. Expanded section of the 85–165 ms TOF window for bn_{90} sample quenched from 450°C, and annealed at 180°C for 11 weeks. In the annealed sample the peak broadening is given by FWHM values of 295.5 ± 2.0 ms and 517.3 ± 21.0 ms for the bornite (084) and digenite (10,10,0) peaks respectively. For the quenched sample the equivalent values are 159.7 ± 1.7 ms and 355.1 ± 14.5 ms.

digenite from the 1*a* -solid solution are extremely rapid.

Diffraction patterns of the visibly exsolved and the rehomogenised and quenched bn_{90} sample are shown in Fig. 7. The important observation regarding these two patterns is that peak intensities in the TOF spectra following both long-term annealing and quenching from 450°C, are essentially the same (allowing for mechanical strain differences discussed in the next section). While these contrasting heat treatments applied to the same sample produced obvious microstructural changes, they resulted in little apparent modification to the modal proportions of coexisting bornite and digenite when measured at room-*T* (Fig. 7). This therefore indicates that precipitation must be essentially complete on quenching as proposed earlier. Despite diffraction measurements being carried out directly after quenching from 450°C, we saw no evidence in the TOF patterns of the 4*a* cubic, metastable supercell described in rapid-quenched samples of this bulk composition by Morimoto and Kullerud (1966). As in the other intermediate compositions examined, the digenite phase in this sample appears to be of the stable 5*a* type on the basis of the relative positions of the (991) supercell peak and the subcell peaks. The digenite (119) peak could not be resolved with any accuracy in this sample due to the low digenite content. The slight shifts in the lattice parameters following rehomogenization of the bn_{90} sample (Fig. 4; Table 2) may be due to minor sulphur losses to the vacuum space on heating the powdered sample.

TABLE 2. Lattice parameters of co-existing bornite and digenite in bulk compositions spanning the bornite-digenite join. Synthetic samples quenched from 600°C, and measured at room-T. Errors in lattice parameters are in the fifth decimal place

Sample	Origin	Bornite			Digenite
		a (Å)	b	c	a (Å)†
bn$_{100}$	Magma Mine, Arizona	10.9500	21.8648	10.9535	–
bn$_{100}$	dry synthetic	10.9495	21.8733	10.9518	–
bn$_{90}$‡	dry synthetic	10.9513	21.8861	10.9560	5.5489
bn$_{90}$*	dry synthetic	10.9491	21.8735	10.9539	5.5468
bn$_{70}$	dry synthetic	10.9485	21.8773	10.9605	5.5536
bn$_{50}$	dry synthetic	10.9699	21.8761	10.9666	5.5531
bn$_{30}$	dry synthetic	10.9922	21.8952	10.9715	5.5535
dg$_{100}$	dry synthetic	–	–	–	5.5560

† Refers to sub-cell edge
‡ Quenched from 450°C
* Annealed at 180°C for 11 weeks

The fact that we observe complete exsolution in even rapidly-quenched digenite-rich compositions where the equilibrium solvus temperature is low, suggests that the free energy of activation barrier to nucleation is not a limiting factor, and may be intrinsically low. However the exsolution process also requires long-range diffusion of cations and vacancies, over length scales of 100's of Å (see next section), in order to produce domains of the two discrete phases, and this must necessarily be rapid at the subsolvus temperatures involved. This suggests that the activation energy for cation diffusion is also low. This has been confirmed by the recent potentiometric experiments performed on bornite and digenite between 5 and 50°C by Bucur and Berger (1995) and Berger and Bucur (1996). Very high Cu diffusion rates were observed, and in the case of bornite, the values measured approached those of fast-ion conductors. Rapid diffusion of Fe ions in the vicinity of the electron beam was observed in TEM studies of bornite by Grace and Putnis (1976), indicating this component is also highly mobile in the sulphur lattice. Although these experimental conditions are not entirely analogous to thermal diffusive processes, they demonstrate the fact that these phases display intrinsically rapid diffusion behaviour, which is presumably facilitated by the high population of vacant tetrahedral sites in their crystal structures. Since the structure of the bornite end-member contains the highest vacancy population of the solid solution (Pierce and Buseck, 1978) we expect this phase to behave as a vacancy sink during exsolution. Total depletion of vacancies from the regions outside of the bornite nuclei does not occur however, since a vacancy population greater than the 10% of the digenite end-member must be present which converges to this value on attainment of equilibrium. It is presumably the presence of these appreciable vacancy populations in both phases that allows transfer of Cu and Fe atoms by diffusional processes to remain rapid at temperatures below the solvus, and prevents quenching-in of the high phase.

Peak broadening and coarsening of exsolved phases

Peak broadening in dg$_{100}$ and the intermediate compositions is quite marked (Fig. 3) with all peak profiles having a significant Lorentzian component, implying the presence of an isotropic lattice strain. This strain can originate from the presence of exsolved domains, induced mechanical strain, or a combination of these factors. In the case of the former effect, it generally follows that the smaller the domain size the larger the broadening effect (David *et al.*, 1988) owing to the greater volume of distorted interface between the coexisting phases. In our case it is impossible to place constraints on the contributions to peak broadening independently without additional structural information, such as TEM images or small-angle scattering data. On the basis of the observed malleability of the synthetic samples, which increases with the digenite content, we tentatively attribute a large component of the observed peak broadening in digenite and digenite-rich compositions to mechanical strain induced during grinding. This property means that a significant component of the mechanical energy used to powder the sample is accommodated in dislocations and other lattice imperfections. However even in bornite-rich compositions there is evidence that mechanical strain is responsible for a major component of the peak broadening. This is well illustrated in Fig. 7 where the TOF spectra of the annealed and optically exsolved bn_{90} sample is shown with that of the same sample after rehomogenization and quenching. Coarsening of exsolution lamellae is a process which is driven by the reduction of lattice strain and the surface energy, since an increase in the mean particle size reduces the volume of strained interface between phases. We would therefore expect a smaller Lorentzian component to the Bragg peaks of the annealed optically-exsolved sample. However in Fig. 7 we see the case is reversed. The peak widths of the exsolved sample are significantly greater than in the quenched sample. This result suggests most of the peak broadening observed in the optically-exsolved sample is due to mechanical strain, induced during grinding. This was ‘annealed out’ on heating of the sample during the subsequent rehomogenization. Evidence for the presence of mechanical strain in powdered natural bornite samples which was subsequently removed during heating was found in a previous HRPD study (Grguric *et al.*, 1998).

Since, as demonstrated, the exsolution process in intermediate compositions is essentially complete on quenching from above the solvus, the growth of optically-visible lamellae seen in Fig. 2 must therefore result from the coarsening of pre-existing sub-microscopic domains of end-member compositions produced during the quenching process. Slight re-adjustments of the compositions of these coexisting domains will have occurred during prolonged annealing at 180°C, since the phase relations at this temperature are somewhat modified from those below 80°C (Grguric, Harrison and Putnis, in prep.). However, the main driving force for microstructural change in this case will have been the reduction in the surface energy, as the thermodynamic requirements for compositional change will have been essentially satisfied. The system achieves this energy reduction via the growth of a small number of large precipitates at the expense of a large number of smaller nuclei. Taking into account both the low Lorentzian broadening component in the bn_{90} diffraction peaks following removal of mechanical strain, and the span of wavelengths of the neutron beam, the lower constraint on the length scales of domains present on quenching would be on the order of 100’s of Å.

Geological implications

Bornite and digenite-bearing assemblages are abundant in many large Cu deposits such as Magma, Arizona (Guilbert and Park, 1986), Butte, Montana (Meyer *et al.*, 1968), and Olympic Dam, Australia (Haynes *et al.*, 1995). Despite fluid inclusion evidence that many of these assemblages were formed at temperatures above the solvus for much of the bornite-digenite series, authenticated occurrences of intermediate compositions of the solid solution are unknown. Furthermore, although the end-members are abundant in these types of deposits, they typically show minimal compositional deviation from stoichiometry (Grguric and Putnis, 1998). This observation holds true for almost all bornite occurrences, with the exception of some low-temperature Red-Bed-type deposits from which sulphur-rich bornites are known (Brett and Yund, 1964). Digenite too shows relatively limited compositional deviation (Morimoto and Gyobu, 1970), however the process of obtaining accurate compositional data on natural samples is frequently hindered by the presence of other Cu-S phases in fine-scale intergrowths (Pósfai and Buseck, 1994). These observations on natural occurrences are consistent with our findings on the exsolution behaviour in the series. We suggest that many of the commonly occurring bornite-digenite intergrowths may well have been deposited as single-phase solid solutions and have subsequently completely exsolved into the end-members on cooling, since as demonstrated, the low kinetic barriers for nucleation of exsolved phases are accompanied by very high diffusion rates at geologically low temperatures.

In addition to the exsolution behaviour, the rapid coarsening kinetics exhibited during prolonged subsolvus annealing of intermediate bulk compositions along the solid solution may eventually lead to the formation of coarse-grained, coalesced intergrowths of bornite and digenite (Brett, 1964) which cannot be positively distinguished from replacement textures and other intergrowths of non-exsolution origin. Natural intergrowths of bornite and digenite exhibiting {100} exsolution microstructures similar to that in Fig. 2 have been described from pegmatites (Ramdohr, 1969), and the Skaergaard Intrusion (Wager *et al.*, 1957; Bird *et al.*, 1991), but in general their occurrence is rare. In the absence of other retarding factors such as high concentrations of impurity atoms (Yund and Hall, 1970) this suggests that the typical cooling rates of ore deposits provide subsolvus annealing for a duration sufficient to advance the coarsening process to the extent that these types of textures are obliterated.

Acknowledgements

The authors wish to thank Kevin Knight and Martin Dove for assistance with neutron diffraction analysis and for many helpful discussions. The helpful comments on a draft manuscript by Richard Harrison were greatly appreciated. We are also grateful for the assistance of Brian Cullum with sample synthesis and Stephen Reed with electron microprobe analysis.

References

Barton, P.B. (1970) *Sulfide Petrology*. Mineral. Soc. Amer. Spec. Papers, **3**, 187–98.

Barton, P.B. and Skinner, B.J. (1979) Sulfide mineral stabilities. In *Geochemistry of Hydrothermal Ore Deposits* (H.L. Barnes, ed.), Wiley, 798 p.

Berger, R. and Bucur, R.V. (1996) Potentiometric measurements of copper diffusion in polycrystalline chalcocite, chalcopyrite and bornite. *Solid State Ionics*, **89**, 269–78.

Bird, D.K., Brooks, C.K., Gannicott, R.A. and Turner, P.A. (1991) A gold-bearing horizon in the Skaergaard intrusion, East-Greenland. *Econ. Geol.*, **86**, 1083–92.

Brett, R. (1964) Experimental data from the system Cu-Fe-S and their bearing on exsolution textures in ores. *Econ. Geol.*, **59**, 1241–69.

Brett, R. and Yund, R.A. (1964) Sulfur-rich bornites. *Amer. Mineral.*, **49**, 1084–98.

Bucur, R.V. and Berger, R. (1995) Electrochemical potentiometric determination of the diffusion coefficient of copper in low digenite, a copper sulfide. *Solid State Ionics*, **76**, 291–6.

David, W.I.F., Akporiaye, D.E., Ibberson, R.M. and Wilson, C.C. (1988) *The high resolution powder diffractometer at ISIS.* ISIS Facility Technical Report, Rutherford-Appleton Laboratory, Chilton, U.K.

van Dyck, D., Conde-Amiano, C. and Amelinckx, S. (1980) The diffraction pattern of crystals presenting a digenite type of disorder. *Physica Status Solidi*, **58**, 451–68.

Grace, J. and Putnis, A. (1976) Thermal decomposition and cation mobility in bornite. *Econ. Geol.*, **71**, 1058–9.

Grguric, B.A. and Putnis, A. (1998) Compositional controls on phase transition temperatures in bornite: a DSC study. *Canad. Mineral.*, **36**, 215–27.

Grguric, B.A., Putnis, A., and Harrison, R.J. (1998) An investigation of the phase transitions in bornite (Cu_5FeS_4) using neutron diffraction and differential scanning calorimetry. *Amer. Mineral.*, **83**, 1231–9.

Guibert, J.M. and Park, C.F. Jr (1986) *The Geology of Ore Deposits*. W.H. Freeman and Co., New York, 985 p.

Haynes, D.W., Cross, K.C., Bills, R.T., and Reed, M.H. (1995) Olympic Dam ore genesis: a fluid mixing model. *Econ. Geol.*, **90**, 281–307.

Holland, T.J.B. and Redfern, S.A.T. (1997) Unit cell refinement from powder diffraction data: the use of regression diagnostics. *Mineral. Mag.*, **61**, 65–77.

Ibberson, R.M., David, W.I.F. and Knight, K.S. (1992) *The high resolution powder diffractometer (HRPD) at ISIS – a user guide*. Rutherford-Appleton Laboratory Report RAL-92-031.

Johnson, M.W. and David, W.I.F. (1985) *The high resolution powder diffractometer at the SNS*. Rutherford-Appleton Laboratory Report RAL-85-112.

Kanazawa, Y., Koto, K., and Morimoto, N. (1978) Bornite (Cu_5FeS_4): stability and crystal structure of the intermediate form. *Canad. Mineral.*, **16**, 397–404.

Knight, K.S. (1996) A neutron powder diffraction determination of the thermal expansion tensor of crocoite ($PbCrO_4$) between 60 K and 290 K. *Mineral. Mag.*, **60**, 963–72.

Koto, K. and Morimoto, N. (1975) Superstructure investigation of bornite, Cu_5FeS_4, by the modified partial Patterson function. *Acta Crystallogr.*, **B31**, 2268–73.

Kullerud, G. (1960) The Cu_9S_5-Cu_5FeS_4 join. *Carnegie Inst. Washington Yearb.*, **59**, 114–6.

Meyer, C., Shea, E.P. and Goddard, C.C. Jr. (1968) Ore deposits at Butte, Montana. In *Ore Deposits of the United States, 1933-1967* (J.D. Ridge, ed.), American Institute of Mining, Metallurgical and Petroleum Engineers, New York.

Morimoto, N. and Gyobu, A. (1971) The composition and stability of digenite. *Amer. Min.*, 56, 1889–909.

Morimoto, N. and Koto, K. (1970) Phase relations of the Cu-S system at low temperatures: stability of anilite. *Amer. Mineral.*, **55**, 106–17.

Morimoto, N. and Kullerud, G. (1961) Polymorphism in bornite. *Amer. Mineral.*, **46**, 1270–82.

Morimoto, N. and Kullerud, G. (1966) Polymorphism on the Cu_5FeS_4-Cu_9S_5 join. *Zeits. Kristallogr.*, **123**, 235–54.

Pierce, L. and Buseck, P.R. (1978) Superstructuring in the bornite-digenite series: a high-resolution electron microscopy study. *Amer. Mineral.*, **63**, 1–16.

Pósfai, M. and Buseck, P.R. (1994) Djurleite, digenite, and chalcocite: intergrowths and transformations. *Amer. Mineral.*, **79**, 308–15.

Putnis, A. and Grace, J. (1976) The transformation behaviour of bornite. *Contrib. Mineral. Petrol.*, **55**, 311–5.

Ramdohr, P. (1969) *The Ore Minerals and Their Intergrowths*. Pergamon Press, 1174 p.

Roseboom, E.H. Jr. (1966) An investigation of the system Cu-S and some natural copper sulfides between 25° and 700°C. *Econ. Geol.*, **61**, 641–72.

Wager, L.R. Vincent, E.A. and Smales, A.A. (1957) Sulphides in the Skaergaard intrusion, East Greenland. *Econ. Geol.*, **52**, 855–903.

Yund, R.A. and Hall, H.T. (1970) Kinetics and mechanism of pyrite exsolution from pyrrhotite. *J. Petrol.*, **11**, 381–404.

[*Manuscript received 16 December 1997:
revised 21 April 1998*]